Environmental Pollution 239 (2018) 532–543

Contents lists available at ScienceDirect

Environmental Pollution

journal homepage: www.elsevier.com/locate/envpol

Exposure to air pollution interacts with obesogenic nutrition to induce tissue-specific response patterns☆

Michal Pardo [a, *], Yael Kuperman [b], Liron Levin [c], Assaf Rudich [d, e], Yulia Haim [d, e], James J. Schauer [f], Alon Chen [g, h], Yinon Rudich [a]

[a] Department of Earth and Planetary Sciences, Weizmann Institute of Science, Rehovot, 76100, Israel
[b] Department of Veterinary Resources, Weizmann Institute of Science, Rehovot, 76100, Israel
[c] Department of Life Sciences, Bioinformatics Core Facility, Ben-Gurion University of the Negev, Beer Sheva, 84103, Israel
[d] The Department of Clinical Biochemistry and Pharmacology, Faculty of Health Sciences, Ben-Gurion University of the Negev, Beer-Sheva 84103, Israel
[e] The National Institute of Biotechnology in the Negev (NIBN), Ben-Gurion University of the Negev, Beer-Sheva 84103, Israel
[f] Environmental Chemistry and Technology Program, University of Wisconsin-Madison, Madison, WI, USA
[g] Department of Neurobiology, Weizmann Institute of Science, Rehovot, 76100, Israel
[h] Department of Stress Neurobiology and Neurogenetics, Max Planck Institute of Psychiatry, Munich, Germany

ARTICLE INFO

Article history:
Received 12 December 2017
Received in revised form
28 March 2018
Accepted 9 April 2018
Available online 21 April 2018

Keywords:
Air pollution
Obesogenic nutrition
Oxidative stress
Inflammation
Lungs
Nrf2 transcription factor
Methyltransferases
Intra-tracheal instillation

ABSTRACT

Obesity and exposure to particular matter (PM) have become two leading global threats to public health. However, the exact mechanisms and tissue-specificity of their health effects are largely unknown. Here we investigate whether a metabolic challenge (early nutritional obesity) synergistically interacts with an environmental challenge (PM exposure) to alter genes representing key response pathways, in a tissue-specific manner. Mice subjected to 7 weeks obesogenic nutrition were exposed every other day during the final week and a half to aqueous extracts of PM collected in the city of London (UK). The expression of 61 selected genes representing key response pathways were investigated in lung, liver, white and brown adipose tissues. Principal component analysis (PCA) revealed distinct patterns of expression changes between the 4 tissues, particularly in the lungs and the liver. Surprisingly, the lung responded to the nutrition challenge. The response of these organs to the PM challenge displayed opposite patterns for some key genes, in particular, those related to the Nrf2 pathway. While the contribution to the variance in gene expression changes in mice exposed to the combined challenge were largely similar among the tissues in PCA1, PCA2 exhibited predominant contribution of inflammatory and oxidative stress responses to the variance in the lungs, and a greater contribution of autophagy genes and MAP kinases in adipose tissues. Possible involvement of alterations in DNA methylation was demonstrated by cell-type-specific responses to a methylation inhibitor. Correspondingly, the DNA methyltransferase Dnmt3a2 increased in the lungs but decreased in the liver, demonstrating potential tissue-differential synergism between nutritional and PM exposure. The results suggest that urban PM, containing dissolved metals, interacts with obesogenic nutrition to regulate diverse response pathways including inflammation and oxidative stress, in a tissue-specific manner. Tissue-differential effects on DNA methylation may underlie tissue-specific responses to key stress-response genes such as catalase and Nrf2.

1. Introduction

Exposure to particulate matter (PM) air pollution and obesity are among the most prevailing global health risks (Chen et al., 2006; Collaborators, 2016; Zanobetti et al., 2014; Yang et al., 2018.). Epidemiological studies in the last decade uncover multi-directional associations between these risk factors. Obese persons (compared to the general population), are more susceptible to air pollution-associated cardiovascular disease (CVD) (Dubowsky et al.,

Abbreviation: PM, particulate matter; HFD, high fat diet; CVD, cardiovascular disease; ROS, reactive oxygen species; GTT, glucose tolerance test; ITT, insulin tolerance test; HPRT, Hypoxanthine Phosphoribosyltransferase 1; TNF-α, tumor necrosis factor α; IL-6, interleukine 6; WAT, white adipose tissue; BAT, brown adipose tissue; IT, intra-tracheal; PC, principal component; MAPK, mitogen-activated protein kinase.

☆ This paper has been recommended for acceptance by David Carpenter.

* Corresponding author.
E-mail address: michal.levin@weizmann.ac.il (M. Pardo).

https://doi.org/10.1016/j.envpol.2018.04.048
0269-7491/

2006), with impaired vascular reactivity, and CVD-associated hospitalizations (Pearson et al., 2010; Zanobetti et al., 2014), as well as higher vulnerability to PM-related respiratory diseases (Dong et al., 2013; McCormack et al., 2015). Indeed, lung exposure to a given PM concentration was higher with increasing weight in children (Bennett and Zeman, 2004). Complementarily, exposure to PM2.5 (2.5 μm diameter particles or smaller, fine particles) was associated with enhanced risk of diabetes incidence and/or to diabetes-associated mortality (Chen and Schwartz, 2008; Collaborators, 2016; Meo et al., 2015; Pearson et al., 2010, Yang et al., 2018). Thus, exposure to air pollution mainly adversely affects the lungs and cardiovascular system, while obesogenic nutrition (high fat diet, HFD) affects classical "metabolic tissues" such as the liver and adipose tissues. However, emerging data suggests that exposure of the lungs to PM, secondarily affects remote tissues' metabolism (Brook et al., 2013; Liu et al., 2013). It was recently shown that PM2.5 exposure induced pulmonary oxidative stress, which induced vascular insulin resistance and inflammation (Haberzettl et al., 2016). Yet, the mechanisms mediating the observed epidemiological evidence for interactions between obesity and lung exposure to air pollution on human health are still poorly understood.

Reactive oxygen species (ROS) regulate different cell processes such as response to stress (Ray et al., 2012), inflammation (Fernandez-Sanchez et al., 2011), cell division (Cui et al., 2015), autophagy (Liu et al., 2015) and more (Giacco and Brownlee, 2010; Lodovici and Bigagli, 2011; Ray et al., 2012; Savini et al., 2013). Evidently, both environmental and metabolic challenges can increase ROS production and lead to oxidative stress, which can affect health. Increased ROS levels can alter metabolic signaling and induce insulin resistance in obese mice (Houstis et al., 2006), and the development of diabetes-related complications (Giacco and Brownlee, 2010). Air pollution can induce adverse health effects by increasing ROS production that contribute to prevailing oxidative stress (Haberzettl et al., 2016; Shuster-Meiseles et al., 2016) and to inflammation (Lodovici and Bigagli, 2011). To maintain redox homeostasis, antioxidant defense genes can be induced by a master transcription factor regulator, Nrf2, and its related genes (Kensler et al., 2007), which are involved in PM-induced health effects (Lin et al., 2016; Lodovici and Bigagli, 2011; Pardo et al., 2015, 2016; Shuster-Meiseles et al., 2016), and in diabetes/obesity development (Giacco and Brownlee, 2010; Haberzettl et al., 2016; Kensler et al., 2007; Kowluru and Mishra, 2017). However, synergism between exposure of the lungs to PM and obesogenic stress through oxidative stress mechanisms and tissue-specific outcomes are not well-understood.

It was hypothesized that obesity is associated with systemic inflammation and increased ROS-induced oxidative stress (Fernandez-Sanchez et al., 2011; McMurray et al., 2016; Savini et al., 2013). In addition, it is evident that deposition of pollution particles in the lungs can provoke not only local, but also systemic effects by releasing signaling agents and soluble components from the respiratory system through the blood system (Kampfrath et al., 2011; Pardo et al., 2016). As we have previously shown that metals from the water soluble PM extracts increased the inflammatory response in mice's lung (Pardo et al., 2016) and the systemic inflammatory response in the blood (Pardo et al., 2016). This, along with the epidemiology-level evidence, suggest possible interactions that may synergize metabolic challenge (such as obesogenic nutrition) with PM exposure (Hooper et al., 2014; Mendez et al., 2013). To address this question, we hypothesized that such interactions may be evident in a tissue-specific manner by investigating the expression levels of genes representing key players and pathways, including Nrf2, antioxidant defense, inflammation and autophagy and apoptosis. Here we challenged this hypothesis by exposure of mice to combined environmental challenges: exposure to extracts from roadside urbans, and an obesogenic diet (total of seven weeks high fat diet, HFD), and studied the expression of selected gene sets in the lungs, liver, white and brown adipose tissues.

2. Materials and methods

2.1. Particulate matter (PM) collection and extracts characterization

Detailed description of the PM sample collection and characterization has been reported previously (Pardo et al., 2015, 2016; Shuster-Meiseles et al., 2016). Briefly, PM3 samples were collected over a period of a week in a roadside monitoring site in central London (Marylebone Road near Baker Street) in spring 2012 using a Hi-Vol sampler (Tisch (TE-230) Hi-Volume Environmental Impactor Sampler). The samplers operated continuously at a nominal flow rate of 1.2 $m^3\ min^{-1}$, and collected about 50–300 mg of PM on mixed-cellulose ester (MCE) filters.

Sections of the MCE filter-collected with PM3 impactor according to the manufacturer's instructions were extracted with high-purity Milli-Q (18 mΩ) water. We consider PM3 to be comparable to PM2.5 (Shuster-Meiseles et al., 2016) (particles of 2.5 μm and smaller, fine particles) rather than the coarse fraction (PM10, particles between 10 and 2.5 μm). Extraction started with 15 min of sonication, followed by 16 h of continuous agitation at room temperature in the dark and then another 15 min sonication. At the end of the extraction period, the suspension was divided to aliquots and distributed for various assays and analyses, (named "PM extract"). Blank samples replicated the processing procedure (named "Control"). The extracts were subjected to a broad range of characterization tools, including: total and water-soluble elements [ICPMS (SF-ICPMS)]; soluble ions (K^+, Na^+, NH_4^+, SO_4^{2-}, NO_3^-, Cl^-) by IC; and soluble organic carbon, as further detailed in (Pardo et al., 2015, 2016).

2.2. Animal studies and exposures

Five weeks old male C57BL/6 mice were purchased from Harlan laboratories (Rehovot, Israel) and maintained in a temperature-controlled room (22 °C) on a reverse 12-h light-dark cycle. The study was approved by The Institutional Animal Care and Use Committee (IACUC) at the Weizmann institute of science. One week after arrival, 40 mice were randomly divided into four groups, two groups were fed *ad libitum* either a high-fat diet (HFD, Research Diets, D12492) and two groups were fed normal-chow diet (Normal chow, NC) until the end of the experiment. On a caloric basis, the HFD consisted of 60% kcal fat, 20% carbohydrate, and 20% protein, whereas the normal diet contained 13.5% kcal fat, 56% carbohydrate, and 30% protein. After 5 weeks on either diet, mice were exposed to water extracts of resuspended PM collected in urban London or to a blank extract using our previously-published protocol (Pardo et al., 2016). A detailed description of the study design appears in Fig. 1. Briefly, mice were exposed every other day for a total of 5 times, using intra-tracheal (IT) administration model (Pardo et al., 2016). The intra-tracheal instillation technique is non-invasive and was proven to be an adequate method to deliver low dose of particles/extracts into the lungs. However, the technique cannot be used to determine the particle deposition patterns in the lungs as would occur following inhalation. In addition, the procedure requires mice to be fully anesthetized, therefore it is difficult to anesthetize the mice everyday as the anesthesia may kill the mice. Each dose of 50 μL of PM water extract corresponded to 10 μg PM. Therefore, a total amount of 50 μg PM was administered during the exposures. The final groups (n = 10 mice/group) were; mice on NC diet that received the blank extract (NC C), mice on NC diet that

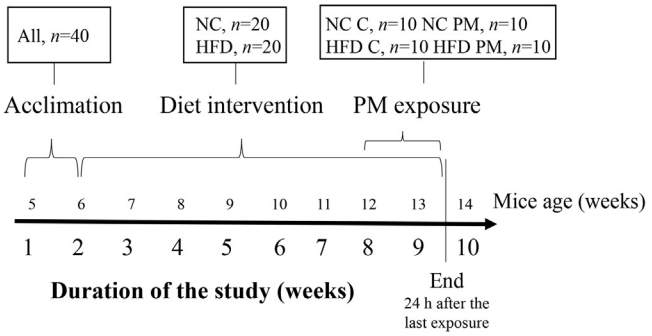

Fig. 1. Study design. Mice were given either normal chow (NC) or high fat diet (HFD) for 5 weeks, and then during additional 2 weeks the mice also received 5 intra-tracheal administrations of either blank or water soluble extract of air pollution samples (PM). The experiment had the following treatment groups: NC C, $n = 10$ NC PM, $n = 10$ HFD C, $n = 10$ HFD PM, $n = 10$.

received PM (NC PM), mice on HF diet that received the blank extract (HFD C), and mice on HF diet that received PM (HFD PM). During the experiment one mouse from the NC PM group died after anesthesia. Body weight was measured once a week. Glucose tolerance test (GTT) and insulin tolerance test were measured before the exposures. Twenty-four hours after the last exposure the mice were scarified with an overdose of ketamine/xylazine. Blood was collected from the orbital sinus right after anesthesia. Serum was obtained, after 15 min incubation at room temperature, followed by clot removal by refrigerated centrifugation at 1000 × g, the serum was immediately kept at −80 °C. Lung, liver, white (epididymal) and brown adipose tissues (WAT and BAT, respectively) were collected. The reasons for selecting these four tissues are: a. The lungs represent a primary exposure organ to air pollution, and in our model, to the intra-tracheal administration of PM extracts. This organ is less responsive to dietary challenges and/or to obesity; b. The liver represents a primary metabolic organ, thus highly responsive to dietary intervention such as obesity, but which also is a major organ for detoxification of xenobiotics; c. White adipose tissue (WAT), the major site of access energy storage, is primarily considered to be responsive to nutritional and energy-balance challenge, and seldom to PM exposure. d. Brown adipose tissue (BAT), a thermogenic adipose and a highly active metabolic organ, particularly in mice housed in typical ambient temperatures that are below thermo-neutrality (~30 °C for mice). Although being primarily a "metabolic organ", BAT was previously proposed to also respond to PM exposure in mice (Xu et al., 2011).

2.3. Glucose tolerance test (GTT) and insulin tolerance test (ITT)

In order to obtain metabolic information, GTT and ITT were assessed before mice were exposed to the soluble extracts of PM. GTT was performed by intra-peritoneum (i.p) injection of (2 g/kg of body weight) glucose after mice fasted for 6 h (5 h of which were of feeding time (darkness) and an hour from their sleeping time (light)). Whole venous blood obtained from the tail vein at 0, 15, 30, 60, 90, and 120 min after the injection was measured for glucose using glucometer (One Touch, Lifescan, Daly,CA). For the ITT, 6 h fasted male mice (5 h of which were of feeding time (darkness) and an hour from their sleeping time (light)) were injected with insulin (0.75 units/kg of body weight, Biological Industries, Beit Haemek, Israel), and blood glucose levels were measured before and at 15, 30, 60, and 90 min after insulin injection (Chen et al., 2006).

2.4. Body composition

Lean and fat body massed were assessed using Echo-MRI (Echo MedicalSystems, Houston, Texas).

2.5. Cytokines measurements

Cytokines were measured in serum. Serum was collected and centrifuged at 500 × g for 15 min at 4 °C, then, transferred to a sterile tube for storage at − 80 °C until assayed. ProcartaPlex Mouse Mix&Match 4-plex was used to detect IL-6, TNF-α, INFγ, and IL1β using Luminex® (Affymetrix, Santa Clara, CA). Each sample was tested in two magnetic beads wells (twice on the plate), and an average result was taken. Calibration curves for each cytokine were performed and the sample measurments were in the linear rage of the assay.

2.6. Gene selection strategy

Specific genes were selected based on their known involvement in various cell responses. Sixty one genes were grouped according to their functional similarity based on the Database for Annotation, Visualization and Integrated Discovery (DAVID) v6.8 (Huang da et al., 2009). The mouse genes were divided into 8 main groups: *(i) "Response to stress"* – a gene-set of 16 genes related to stress response and the activation of nuclear factor-erythroid 2 (Nrf2) pathway. Nrf2 is a transcription factor that binds to antioxidant response elements (ARE) and activates transcription of phase II protective genes (Deng et al., 2013; Jimenez-Osorio et al., 2015; Zhang et al., 2012) such as *ho-1, gclc, gclm,* and *nqo1*. Also included are genes involved in ROS metabolism, such as oxidative stress responsive genes (*cat, gsr, gpx-1*) and genes associated with superoxidemetabolism such as superoxide dismutases (SOD). *(ii)* "*Apoptosis*" *group* profiles the expression of 4 key genes involved in the regulation of apoptosis (*bcl2, bcl-xlL*), the other genes are related to the caspases family. *(iii) "Autophagy"* (a lysosomal degradative pathway for intracellular components) profiles 8 genes related to vacuole formation (*atg12, atg5, atg7, beclin1*) and to the transition from autophagosome to lysosome (*dram1*). *(iv) "Lysosomal" group* included acidic proteases (*cathepsin B* and *D*), transcription factor controlling lysosomal biogenesis (*tfeb*) and lysosomal structural proteins (*lamp2*). *(v) "Inflammation and/immune response"* – is profiled by the expression of genes mediating inflammatory response such as cytokines (*il6, il1β, Il1rn)* and the regulation of the inflammatory response such as *tlr2, tlr4*, *nos2* and *nfkb1,* also included genes controlled by TNF ligand and TNF receptor signaling pathways. *(vi) "MAP kinases"* - includes 11 genes related to the map kinase signaling pathway. *(vii) "Mitochondria" group* included genes related to the mitochondria energy metabolism (*atp5a1, idh1, sdhb*). *(viii) "Heat shock"* - HSP set containing *hsp8* and *hsp1b* proteins that function as chaperones. "Others" represents all the remaining genes that were not statistically significant. All the gene information, full names and clusters are detailed in Table 1. While some genes may be related to more than one cluster, this functional classification was kept throughout the analysis and maintained in order to highlight the general changes in gene expression among the different treatments and tissues.

2.7. mRNA extraction, microfluidics DNA analysis and qPCR

Total RNA was extracted from the lungs, liver, WAT and BAT using TRI reagent according to manufacturer's recommendation. Dnase I (Invitrogen) was applied prior to reverse transcriptase procedure. Total RNA (1 μg) was reverse-transcribed to cDNA using random hexamers (ABI, California, USA). Fluidigm Digital Array IFC

Table 1
Summary table for genes information used in the analysis. The table contains information for the common genes used, their full names, ID number, group cluster, and primers sequence. Several genes had more than one primer sequence, these genes are numbered under the gene symbol column.

Name	Gene ID	Forward 5'to'3	Reverse 5'to'3
Gene Group 1 Response to stress			
superoxide dismutase 2, mitochondrial(Sod2)	20656	CCATTTTCTGGACAAACCTG	GACCTTGCTCCTTATTGAAG
glutathione reductase(Gsr)	14782	GTTCACACAGGTTAAGGAAG	TATTCAGATTCAGGCCCTTAG
NAD(P)H dehydrogenase, quinone 1(Nqo1)	18104	AGCTGGAAGCTGCAGACCTG	CCTTTCAGAATGGCTGGCA
		TATTTCAGTTCCCATTGCAG	GTGATAGAAAGCAAGGTCTTC
superoxide dismutase 1, soluble(Sod1)	20655	CACTCTAAGAAACATGGTGG	GATCACACGATCTTCAATGG
catalase(Cat)	12359	CTCCATCAGGTTTCTTTCTTC	CAACAGGCAAGTTTTTGATG
		CCGACCAGGGCATCAAAA	GAGGCCATAATCCGGATCTTC
glutathione peroxidase 1(Gpx1)	14775	TGGCTTGGTCATTCTGGGC	CCCACCTGGTCGAACATACTT
heme oxygenase 1(Hmox1)	15368	CATGAAGAACTTTCAGAAGGG	TAGATATGGTACAAGGAAGCC
		CTGGTGATGGCTTCCTTGTA	GGCATAGACTGGGTTCTGCT
nuclear factor, erythroid derived 2, like 2(Nfe2l2)	18024	TCTCCTCGCTGGAAAAAGAA	AATGTGCTGGCTGTGCTTTA
nuclear factor erythroid 2–related factor 2		CAGAGACATTCCCATTTGTAG	ATTCGGGAATGGAAAATAGC
glutamate-cysteine ligase, catalytic subunit(Gclc)	14629	CTATCTGCCCAATTGTTATGG	ACAGGTAGCTATCTATTGAGTC
glutamate-cysteine ligase, modifier subunit(Gclm)	14630	GCACAGGTAAAACCCAATAG	TTAGCAAAGGCAGTCCCTC
metallothionein 2	17750	TGTACTTCCTGCAAGAAAAG	GGCTTCTACATGGTCTATTTAC
Group 2 Map signaling			
mitogen-activated protein kinase kinase 4(Map2k4)	26398	CTAACACAAGTGGTGAAAGG	ACCTCTACAGTACGTTCTTC
thymoma viral proto-oncogene 2(Akt2)	11652	GAAAGGAGACTGTAAAAAGTGG	ATACAGTATCGTCTTGGGTC
insulin receptor substrate 1(Irs1)	16367	GATCGTCAATAGCGTAACTG	ATCGTACCATCTACTGAAGAG
thymoma viral proto-oncogene 1(Akt1)	11651	TGATCAAGTTCTCCTACTCAG	TCCGAGAAACAAAACATCAG
mitogen-activated protein kinase 14(Mapk14)	26416	CTGGTACAGACCATATTAACC	GCATCCTGTTAATGAGATAAGC
mitogen-activated protein kinase 1(Mapk1)	26413	CAGTATTATGACCCAAGTGATG	CCTTGTCCTGACCAATTTAAG
receptor (TNFRSF)-interacting serine-threonine kinase 1(Ripk1)	19766	TATGTAGAAGAGGATGTGGC	TCCAGGTTGTTCTGAATTTG
mitogen-activated protein kinase kinase kinase 5(Map3k5)	26408	GGCCGAATCTACAAAGATATG	CTTTTTGAACCAAGATGCTC
nuclear factor of kappa light polypeptide gene enhancer in B cells 1, p105(Nfkb1)	18033	ATCTATGATAGCAAAGCCCC	TGGATGTCATCTTTCTGAAC
unc-51 like kinase 1(Ulk1)	22241	AGATTGCTGACTTTGGATTC	AGCCATGTACATAGGAGAAC
FBJ osteosarcoma oncogene(Fos)	14281	AGATTGCTGACTTTGGATTC	AGCCATGTACATAGGAGAAC
pyruvat kinase	18746	CAGGTTTGATGAGATCTTGG	CTTCTTGATCATGCTCTCC
Gene Group 3 Inflammatory immune/response			
tumor necrosis factor receptor superfamily, member 25	85030	ATCTGTGCATATTGTCGATG	GACAGTGGTACAGATTTTCC
interleukin 1 beta(Il1b)	16176	GGATGATGATGATAACCTGC	CATGGAGAATATCACTTGTTGG
tumor necrosis factor(Tnf)	21926	GGTTATCTTGCTAGGTCTTTG	GATCCCTACAAATGATGGAG
toll-like receptor 2(Tlr2)	24088	CTAGAAGTGGAAAAGATGTCG	TAGCATCCTCTGAGATTTGAC
Fas ligand (TNF superfamily, member 6) (Fasl)	14103	TGAAAAGGCAAATAGCCAACC	TATACTTCACTCCAGAGATCAG
Fas (TNF receptor superfamily member 6) (Fas)	14102	TGAATGCCTCAAATCTTAGC	TTTTAGCTTCCTGGATTGTC
		TGAATGCCTCAAATCTTAGC	TTTTAGCTTCCTGGATTGTC
toll-like receptor 4(Tlr4)	21898	GATCAGAAACTCAGCAAAGTC	TGTTTCAATTTCACACCTGG
interleukin 6(Il6)	16193	AAGAAATGATGGATGCTACC	GAGTTTCTGTATCTCTCTGAAG
tumor necrosis factor (ligand) superfamily, member 10(Tnfsf10)	22035	AATTCCAATCTCCAAGGATG	GAATAGATGTAATACAGGCCC
tumor necrosis factor (ligand) superfamily, member 15(Tnfsf15)	326623	TAACAGAAGAGAGATCTGAGC	TTCTTAATTGTCAGGTGTGC
tumor necrosis factor receptor superfamily, member 9(Tnfrsf9)	21942	ACATTTAATGACCAGAACGG	CTTCTTAAATGCTGGTCCTC
nitric oxide synthase 2, inducible(Nos2)	18126	CATCAACCAGTATTATGGCTC	TTCCTTTGTTACAGCTTCC
interleukin 1 receptor antagonist(Il1rn)	16181	CAGAAGACCTTTTACCTGAG	GGCACCATGTCTATCTTTTC
nuclear factor of kappa light polypeptide gene enhancer in B cells 1, p105(Nfkb1)	18033	ATCTATGATAGCAAAGCCCC	TGGATGTCATCTTTCTGAAC
Gene Group 4 Autophagy			
beclin 1, autophagy related(Becn1)	56208	CAATAATTTCAGACTGGGTAG	ATTTGTCTGTCAGAGACTCC
autophagy related 12(Atg12)	67526	CTCTATATGAGTGTTTTGGCAG	TTGATAGTAAGTCTCTTCCCAC
autophagy related 7(Atg7)	74244	CTGTTCACCCAAAGTTCTTG	TCTAAGAAGGAATGTGAGGAG
autophagy related 5(Atg5)	11793	TAGAATATATCAGACCACGACG	CTCCTCTTCTCTCCATCTTC
DNA-damage regulated autophagy modulator 1(Dram1)	71712	TATATATCACGTGGTGAGCG	GTGACACTCTGGAAATCTTG
E2F transcription factor 1(E2f1)	13555	CAGAACAGATGGTCATAGTG	GAGATCTGAAATGTCTCTGAAG
		ATGGGTGATACCTTAAGTCC	GTACAAAGGGACTGTTTCTC
		CAGAACAGATGGTCATAGTG	GAGATCTGAAATGTCTCTGAAG
sequestosome 1/p62	18412	AATGTGATCTGTGATGGTTG	GAGAGAAGCTATCAGAGAGG
Gene Group5 Apoptosis			
caspase 1(Casp1)	12362	GGGACATTAAACGAAGAATCC	GGAAGTATTGGCTTCTTATTGG
caspase 9(Casp9)	12371	TGATCGAGGATATTCAGCAG	CCTCTAAGCAGGAGATGAAG
B cell leukemia/lymphoma 2(Bcl2)	12043	ATGACTGAGTACCTGAACC	ATATAGTTCCACAAAGGCATC
BCL2-like 1(Bcl2l1)	12048	GCTTGGATAATGAGACAAG	GAGAACATTCAGACCACAAG
Gene Group 6 Lysosomal			
cathepsin D(Ctsd)	13033	GTATATACTCAAGGTATCGAG	CCTATTGTTGTCTCTGTCAAAC
cathepsin B(Ctsb)	13030	AGGTGGAGTCTACAATTCTC	GTGTACCCAAAGTGCTTATC
lysosomal-associated membrane protein 2(Lamp2)	16784	CTAATGGCTCAGCTTTCAAC	AAAGGTGTTGATCTGAAACG
transcription factor EB(Tfeb)	21425	ACTATGATGGGGAAGAACAG	GGTACTTGTACCTCCTTCTC
Gene Group 7 HSP			
heat shock protein 8(Hspa8)	15481	CACAGAGAGATTAATTGGGG	GTTTGGCATCAAAAACTGTG
heat shock protein 1B(Hspa1b)	15511	AAACAGACTCTTTGCACTTG	TAACAGTCAACGCAATTACC
Gene Group 8 Mitochondria			
succinate dehydrogenase complex, subunit B, iron sulfur (Ip) (Sdhb)	67680	TCTTGTAGAGAAGGCATCTG	GACTAGATCCTTGATCACATAC
ATP synthase, H+ transporting, mitochondrial F1 complex, alpha subunit 1(Atp5a1)	11946	AATGCTATTGATGGAAAGGG	CAATCGATGTTTTCCCAGTC
isocitrate dehydrogenase 1 (NADP+), soluble(Idh1)	15926	ACAGAGCAAAGCTTGATAAC	GTCAGAACGTTGTACATTGG

(*continued on next page*)

Table 1 (*continued*)

Name	Gene ID	Forward 5'to'3	Reverse 5'to'3
glucose-6-phosphatase, catalytic	14377	TTCAAGTGGATTCTGTTTGG	AGATAGCAAGAGTAGAAGTGAC
cytochrome *c* oxidase subunit IV isoform 1	12857	AGAAGAGCTATGTGTATGGC	CTTCTTCCACTCATTCTTGTC
Gene Group 9 Controls			
β-actin	11461	GATGTATGAAGGCTTTGGTC	TGTGCACTTTTATTGGTCTC
		TTCTACAATGAGCTGCGTGTG	GGGGTGTTGAAGGTCTCAAA
β-tubolin	22152	CAACTATGTAGGGGACTCAG	CCACTCTGACCAAAGATAAAG
ribosomal protein, large, P0	11837	CTTCTCCTATAAAAGGCACAC	AAAGTTGGATGATCTTGAGG
		AACCGCTACTGTTTACTTTG	TCACACCTGGAAAATCTTTG
18 s subunit	19791	ACGGAAGGGCACCACCAGGA	CACCACCACCCACGGAATCG

nanofluidic biochip technology was used to profile selected genes related to several signaling pathways as detailed next. Pre-amplification was performed with PreAmp Master Mix (Fluidigm) and a pool of the 96 designed primers followed by an exonuclease treatment (Fluidigm Corporation). Pre-amplified cDNA was then used for high-throughput qPCR measurement of each amplicon using a BioMark HD system. Briefly, each amplified cDNA was mixed with 2X SsoFast EvaGreen Supermix with Low ROX (Bio-Rad) and 20X DNA Binding Dye Sample Loading Reagent (Fluidigm). Sample mix was then pipetted into one sample inlet in a 96.96 Dynamic Array IFC chip (Fluidigm). Individual primer pairs (50μM, Table 1.) were mixed with Assay Loading Reagent (Fluidigm) and Low TE. The mix was pipetted into one assay inlet in the same Dynamic Array IFC chip. Quantitive PCR (qPCR) was performed on the BioMark HD real-time PCR reader (Fluidigm) following manufacturer's instructions using standard fast cycling conditions and melt-curve analysis, generating an amplification curve for each gene of interest in each cell. Data were analyzed using Real-time PCR Analysis software (Fluidigm) (Fischer et al., 2016).

For internal validation of the microfluidics assay, several key genes were assessed with two different primer sets. Gene information, full names and primers sequence are detailed in Table 1. Endogenous control genes were chosen as previously indicated (Kozera and Rapacz, 2013; Matouskova et al., 2014; Nygard et al., 2007), and their Δct were between 0.5 and 1 cycles among samples. Normalization was performed with two different set of primers, the lung and liver genes were normalized to two different sets of β-Actin primers, and the WAT and BAT genes were normalized to two sets of Rplp0 and β-Actin (to reduce variation that may occur with a single normalizer).

For quantification of mRNA expression (*Mus musculus*, DNA methylation and homo sapiens, Nrf2 and related-genes), real-time PCR was performed using the Fast SYBR Green PCR mix (Applied Biosystems, Foster City, CA, USA) in StepOnePlus RT PCR instrument. The following cycling conditions were used: 40 cycles at 95 °C for 30 s and 60 °C for 30 s and extension at 72 °C for 30 s. Relative gene expression was obtained after normalization to the endogenous control genes (β-Actin and HPRT) using $2^{-\Delta\Delta Ct}$ formula. Primers sequence are detailed in Table 2.

2.8. Cell cultures

Human tumorigenic lung epithelial (A549 cells) and human liver hepatocellular carcinoma HepG2 cell lines were grown in RPMI-1640 supplemented with 10% fetal calf serum, and penicillin-streptomycin 1% (w/v). The cultures were grown at 37 °C in a humidified atmosphere consisting of 95% air and 5% CO_2.

2.9. 5Aza-dC treatment of cells

Six hours before treatment, 100,000 cells/well were seeded. Then, cells were treated with 5-aza-2′-deoxycytidine (5Aza-dC, Sigma) for 72 h at concentrations of 0.5, 2 and 10 μM. After incubation, RNA was extracted from human A549 and HepG2 cells as previously described. Quantitive PCR (qPCR) was performed for selected genes.

2.10. Strategy for gene expression analysis and statistical analysis

Two chips for the Fluidigm Digital Array IFC nanofluidic biochip technology were prepared (for the lung, liver, and adipose tissues) and were analyzed together. The two chips contained the same number of genes; the chip containing the lung and liver samples examined 62 genes, and the chip containing the adipose tissues examined the same 62 genes with additional genes relevant for the adipose tissues. A complete statistical analysis was conducted for the common genes (Table 1).

Log 2 transformation was not performed since the data was already normalized to relative quantification values with $2^{-\Delta\Delta Ct}$. Technical replicates were averaged both on the sample level (samples were tested in duplicates) and on the gene level (on key genes that were tested twice). Notably, different primers for the same gene were analyzed as if they were separate genes as they may reflect various gene isoforms. For each independent tissue

Table 2
List of *Mus musculus* and *Homo sapiens* primers sequence.

Name and species		Forward 5'to'3	Reverse 5'to'3
DNA methyl transferase 3a1, mus musculus	ID: 13435	CCTAGTTCCGTGGCTACGAGGAGAA	TCTCTCTCCTCTGCAGCCGACTCA
DNA methyl transferase 3a2, mus musculus		GCAGCTATTTACAGAGCTTC	TCCTCCACCTTCTGAGACT
DNA methyl transferase 3b, mus musculus	ID: 13436	TTCAGTGACCAGTCCTCAGACACGAA	TCAGAAGGCTGGAGACCTCCCTCTT
DNA methyl transferase 1, mus musculus	ID: 13433	CCTAGTTCCGTGGCTACGAGGAGAA	TCTCTCTCCTCTGCAGCCGACTCA
Hypoxanthine Phosphoribosyltransferase 1, mus musculus	ID: 15452	GCAGTACAGCCCCAAAATGG	GGTCCTTTTCACCAGCAAGCT
β-actin, mus musculus	ID: 11461	GATGTATGAAGGCTTTGGTC	TGTGCACTTTTATTGGTCTC
nuclear factor, erythroid derived 2, like 2(Nfe2l2), homo sapiens	ID: 4780	CAACCCTTGTCACCATCTCA	GTGTTCTCACATTGGGCATC
heme oxygenase 1(Hmox1), homo sapiens	ID: 3162	GAGAAAGCAAGTGGCTCACC	TGACGGACCTGGTTCTTACC
catalase(Cat), homo sapiens	ID: 847	TTCTTGGATGCAAAGTGCTG	GTCAGCTGAACCCGATTCTC
glutathione peroxidase 1(Gpx1), homo sapiens	ID: 2876	CTGGTCCTGTTGATCCCAGT	CTGACACCCGGCACTTTATT
Hypoxanthine Phosphoribosyltransferase 1, homo sapiens	ID: 3251	TGTGGTATGGTATGGCTTGC	GGTGAAAGAGCAGGTGAACA
β-actin, homo sapiens	ID: 60	TCGTGCGTGACATTAAGGAG	CCATCTCTTGCTCGAAGTCC

analysis, genes with no variance (variance = 0) were discarded. The BAT analysis was based on 4 animals only, due to one outlier.

Principal component analysis (PCA) plots and the statistical contribution of the genes to the principal components were generated using the "FactoMineR" R package. To identify genes with statistically significant interaction between "diet" and "PM treatment", an ANOVA test was performed using the following model:

Expression ~ (Diet + Treatment + Diet)/Treatment.

The interaction P values were corrected for multiple testing according to Hochberg (1988) and were implemented using the "p.adjust" R function. Genes that presented significant interaction (adjusted p values < 0.05) were hierarchically clustered and divided into discrete clusters using the "eclust" function from the "factoextra" R package while using "Euclidean" metric to calculate the dissimilarities between observations and the "complete" agglomeration method.

The metabolic measurements, cytokines, DNA methyltransferases and the 5 Aza-dC experiments are presented as mean ± SEM. Statistical analyses were performed using *t* tests or one-way ANOVA using the Fisher protected least-significant difference method. Statistical evaluation was performed with OriginLab (Data Analysis and Graphing Software, Northampton, MA, USA). The level of significance was set at $P < 0.05$.

3. Results

3.1. Environmental characterization

The PM3 sample from London was the dominant fraction of the total PM, with PM3 concentration of 51.5 μg m^{-3}, this measured PM concentrations are above the European PM standards (annual average of 25 μg m^{-3} for PM2.5). The coarse fraction accounted for about 10% of the total collected mass (Shuster-Meiseles et al., 2016). Metals analysis in ICP-MS included all of the quantified elements (Li, B, P, V, Cr, Co, Ni, Cu, Zn, As, Se, Sr, Y, Nb, Mo, Rh, Pd, Cd, Sn, Sb, Cs, Ba, La, Ce, Pr, Nd, Sm, Eu Dy, Ho, Yb, Lu, W, Pt, Tl, Pb, Th, and U), excluding those assigned to dust (i.e. Al, Ca, Fe, Mn, Rb, Sc, and Ti). In the fine PM, 40% of the mass fraction was nitrate. The contribution of fine particles to the ambient concentration of metals in the roadway samples was typically greater than that of the larger particles. In the London sample the metals in fine fraction was higher than the coarse fraction (0.6 and 0.3 μg m^{-3}, respectively).

Mice were exposed to aqueous extracts of 10 μg PM3 at each exposure (with a total of 5 exposures). The average concentration of a daily 10 μg exposure for a mouse would be equivalent to a concentration of about 230 μg m^{-3} for humans (Bide et al., 1997). Such concentration would be in the upper end of urban pollution in Asia and in the range of indoor pollution impacted by unvented solid fuel burning, as well as in occupational exposures.

3.2. Metabolic characterization

To examine possible tissue-specific interactions between obesogenic diet and exposure to pollution, mice were kept on HFD for 5 weeks before exposure. As expected, mice on HFD exhibited increased adiposity and were dys-glycemic compared to mice on normal chow (NC) diet. This was manifested by increased body weight (Fig. 2A and S1A), elevated plasma glucose (Fig. 2B and S1B), insulin levels (Fig. 2C and S1C), and altered body composition analysis (Fig. 2D and S1D). The metabolic changes observed in our study resemble in magnitude to changes observed in other studies on 6 weeks HFD-treated mice (Axelsen et al., 2015; Fisher-Wellman et al., 2016), and may represent an early, rather than a long-term or chronic state of obesity. Importantly, exposure to PM solely did not influence body mass composition (Fig. 2E) or body weight (Fig. S1A). However, fed-state glucose levels slightly increased in the HFD PM group (Fig. 2F). Since the exposures were performed every other day, it was impossible to examine GTT and ITT during or at the end of the exposures as the anesthesia and the stress of the mice may change the measured levels of GTT and ITT. For this reason the GTT and ITT data is obtained only before the exposures. We have therefore tested the fed glucose levels and body mass composition in order to obtain some indication on the mice' metabolic state. Body mass composition was measured before and after the exposures since this examination is not invasive.

To assess systemic inflammation, which may be driven by exposure to either the HFD and/or the pollution, circulating levels of four prototypical pro-inflammatory cytokines were measured in serum at the end of the experiment. Interestingly, here we found a predominant effect of the PM exposure, with a 2–4-fold elevation in both TNF-α and IL-6 levels, regardless of the diet (Fig. 2G). IL-1β and INF-γ did not exhibit significant difference between the 4 intervention groups, and the lack of elevated levels in response to HFD alone is likely attributed to the relatively short, 7-week long diet or to the relatively young age of the mice.

3.3. Organ-specific changes in expression of selected genes following diet and PM challenges

To assess whether interaction exists between the HFD and PM exposure challenges, we investigated changes in gene expression of several selected pathways, in the 4 different tissues. Principal component analysis (PCA) for the four treatment groups was used to assess the overall similarity between samples, and is presented in Fig. 3 (A to D). Interestingly, the PCA distinguished between the 4 treatment groups, particularly the lungs and the liver. Intriguingly, the lung tissue was markedly responsive to the dietary challenge (compare NC C to HFD C), and the liver was highly responsive to the PM exposure (compare NC C to NC PM, and HFD C to HFD PM, Fig. 3). Segregation of the 4 groups was less robust for the two adipose tissues, partially because of higher variability between individual samples in each group (see BAT NC PM and WAT HFD PM). Such inter-individual variability is consistent with previous reports that examined the physiological responses of mice to HFD intervention (Montgomery et al., 2013). Nevertheless, the potential for an interaction in the gene responses to PM and dietary challenges is readily seen in the lungs, liver and BAT (note a distinctly separable cluster of the HFD PM group).

The relative contributions of the gene groups to the variance in PC1 (Fig. S1) and PC2 (Fig. 3E–I) is represented by pie charts for mice receiving the combined nutrition-PM challenge (HFD PM). Genes with the largest variation in the PCA graphs (p value < 0.05) were grouped according to their functional clustering (as appears in Table 1). For PC1, the contribution of the different gene families was rather similar among the tissues and resembled the relative initial distribution of the gene groups ("Native", Fig. S2). As for PC2 (Fig. 3E–I): in the lung, the primary organ of exposure, the "Inflammatory/immune response" and "Response to stress" genes dominated the contribution to the variability (Fig. 3E). In the liver, an organ which receives secondary exposure, activated genes in the HFD PM group were mainly attributed to the "Inflammatory/immune response" and "Response to stress genes" but also to the "Lysosomal and MAP kinase" genes (Fig. 3G). The brown adipose tissue (BAT) showed a substantial increase in the contribution of "Response to stress" genes (Fig. 3H), and in the white adipose tissue (WAT) a predominant increase in genes related to "MAP kinase signaling" and to "Autophagy" clusters was observed (Fig. 3I). Thus, organ-specific gene alteration patterns in the HFD PM group are

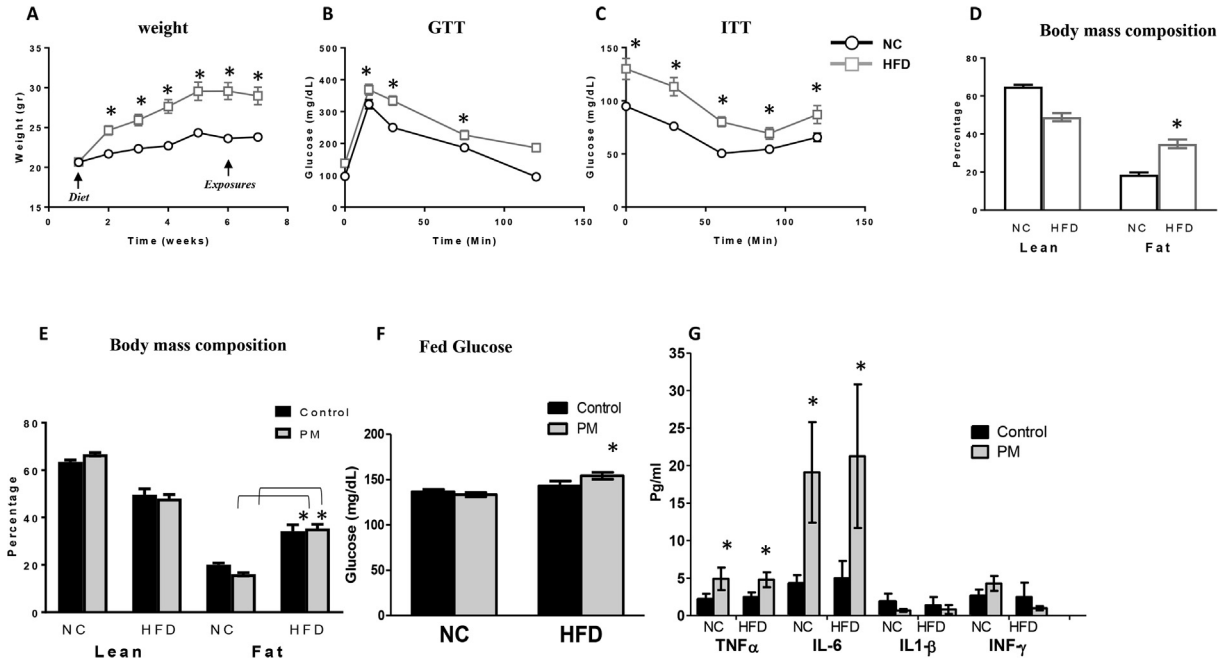

Fig. 2. Metabolic parameters and cytokine measurements in the study groups. Mice weights (A) are shown from the beginning of the intervention (i.e., at 6 weeks of age, week 1) till the end of the intervention – week 7. Black arrows in the graph indicate the study time line; Diet indicates the beginning of the diet intervention and exposures indicates when the exposures started with respect to the duration of the study. After five weeks of diet and before the exposures several metabolic tests were performed in order to perceive the influence of the diet (after 5 weeks on the diet), upper panel; Glucose tolerance test, GTT (B) and Insulin tolerance test, ITT (C) Body mass composition (D). Lower panel metabolic testes performed after the exposures (after 7 weeks on the diet) body mass composition (E), fed glucose (F), and Cytokine measurements from serum (G). N = 10, Data are means ± SEM. * significantly higher at $p < 0.05$ than NC C– the control.

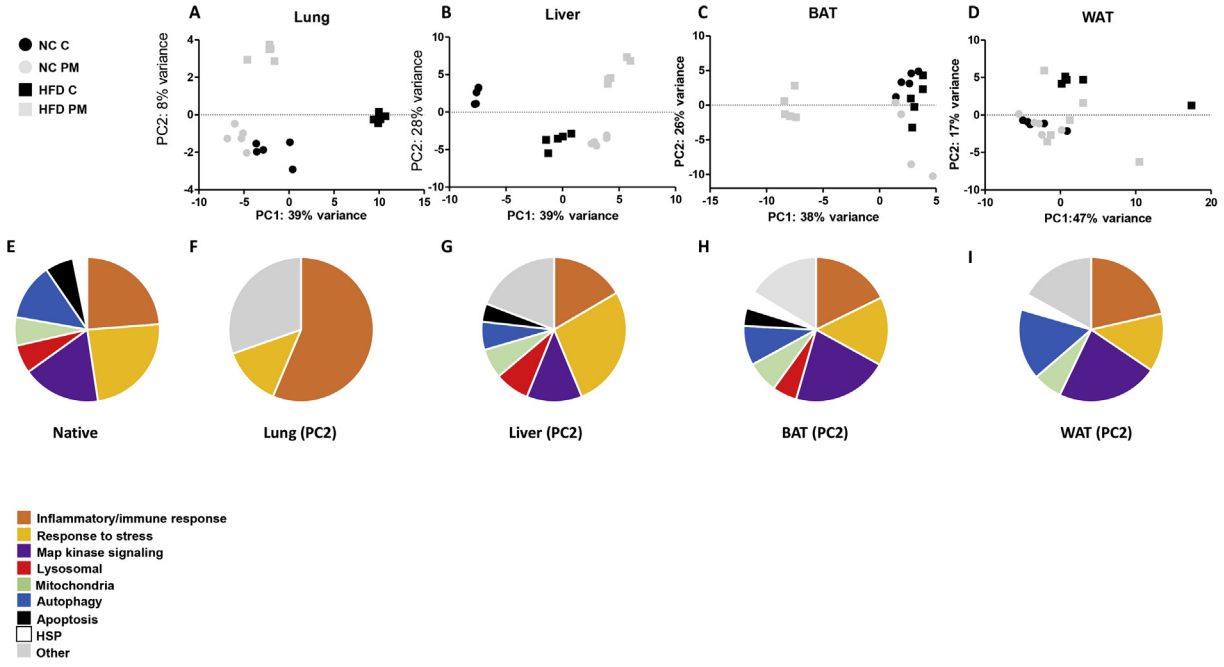

Fig. 3. Principal component analysis (PCA) plots and gene grouping for the expression of genes in the lung, liver, BAT and WAT tissues. The samples are plotted in a two-dimensional space (PC1 and PC2), capturing most of the variance in the dataset. Each mouse is represented by a single color coded shape. The genes used for analysis were grouped according to their function and gene ontology (detailed in Methods section), with a relative distribution as shown in the "Native" pie chart (*E*). Pie charts demonstrate the relative contribution of the major gene groups contributing to the variance between samples in PC2 (*F, G, H, I*) in a tissue-specific manner.

more clearly reflected in the gene groups of PC2 than in PC1.

To identify patterns of change in gene expression that reflect interaction between the combined exposure to both obesogenic diet and to PM extracts (Figs. S3A–D; left panel), heat map presentation for each tissue was used (Genes with P value < 0.05 in each tissue are presented). The statistical analysis was performed in an unbiased manner to identify clusters of genes that exhibit unique patterns of interaction in the response to both challenges

(for more details on the statistical approach to define interaction see Methods).

Genes exhibiting synergism between HFD and PM for all tissues examined are presented in Fig. 4; in the lung, a synergistic effect was best reflected in a cluster that included *tlr2, tlr4* and *il-ra*, all closely related to the "Inflammatory/immune response" group (Fig. 4A). In the liver (Fig. 4B), synergism of the diet and PM was observed with clusters that included genes comprising the "Response to stress", "Autophagy" and "Inflammation" groups, in some cases exhibiting the opposite pattern to that seen in the lung (example: *atg12, lamp2*). In the liver, the strongest increase in response to the combined HFD-PM challenge was observed in the expression of the heavy metals binding protein metalothioneine-2 (*mt-2*). In BAT (Fig. 4C), clusters included genes that similarly behaved in either the lung (*tlr4*) or the liver (*il1β, ho-1, gpx-1*). In WAT *ho-1* was the only gene that demonstrated a synergistic response to the two environmental challenges (Fig. 4D). Collectively, gene expression response patterns were highly tissue-specific, including inflammatory genes in the lung, inflammatory, autophagy and stress response in the liver, inflammatory, stress response and apoptosis in BAT, and only *ho-1* in WAT.

3.4. Potential involvement of altered DNA methylation

The contrasting response in the "response to stress" cluster in the lung and liver suggest a putative role for a high-level gene regulation control mechanism that was tissue-specific. One such mechanisms is gross demethylation of the genome. DNA methylation has been shown to regulate biological processes, such as inflammation, immune response, and oxidative stress (Cantone et al., 2017; Yara et al., 2015). To test this hypothesis, we treated A549 lung epithelial cells and HepG2 liver carcinoma cells with varying concentrations of 5Aza-dC (an agent used to remove methyl groups from DNA by inhibiting DNA methyltransferase). After 72 h of constant exposure to 10 mM 5Aza-dC, we analyzed the cells for *catalase, ho-1, gpx-1* and *Nrf2* mRNA levels. The complete set of data with 5Aza-dC dose dependent concentration is shown in Fig. S4. The level of *catalase* increased at the highest concentration following 72 h of treatment of 5Aza-dC in the lung A549 cells, but decreased in HepG2 liver cells (Fig. 4A and E, respectively). *ho-1* did not change in A549 cells following 5Aza-dC treatment whereas its mRNA levels decreased in HepG2 cells following the treatment (Fig. 5B and F, respectively). *gpx-1* levels increased significantly in A549 and HepG2 cells (Fig. 5C and G, respectively), and *Nrf2* levels decreased in both A549 and HepG2 cells (Fig. 5D and H, respectively). These results suggest that the expression of these genes is influenced by DNA methylation in a gene and tissue -specific manner. Furthermore, the inverse trends of *catalase* and *ho-1* are in accordance with our *in vivo* findings in the lung and liver in response to dietary and PM exposure challenges (Fig. 5). Collectively, these results suggest a potential involvement of exposure-related, tissue-specific alterations in DNA methylation, which could underlie the gene expression findings.

We have therefore examined the expression of several DNA methyl transferases in the lung and liver of the four mice groups. This family of enzymes has an essential role in *de novo* methylation and is involved in mouse development (Okano et al., 1999). Intriguingly, in the lung (Fig. 5A), *dnmt3a2* increased after exposure to PM, and this effect was synergistically augmented with the combined exposure to HFD and PM (Fig. 5A). Yet, in the liver (Fig. 5B), a different behavior was observed for *dnmt3a2* expression; HFD increased *dnmt3a2* expression whereas PM decreased it (Fig. 5B). No changes were observed in *dnmt3a1*, *dnmt3b* and *dnmt1* in either lung or liver (see Fig. S5).

4. Discussion

Obesity and exposure to air pollution contribute to the rising burden of human health risks globally (Collaborators, 2016; Yang et al., 2018). In this study, we investigated possible synergism between exposure to PM pollution and the early effects of exposure to an obesogenic diet. Our study shows that the gene expression profile is substantially different when mice are exposed to water soluble PM extracts on the background of regular versus obesogenic diet, and importantly, this response is organ-specific. Importantly, the synergistic effects of both stressors are not universally overt, but may involve defined pathways in specific organs, potentially uncovering tissue-selective targets when considering the development of novel therapeutic/preventive approaches to alleviate the negative impacts of air pollution and obesogenic stressors on health.

Obesity or metabolic syndrome increase inflammation, where fat tissues secrete numerous hormones and cytokines such as IL-6 and TNF-α (Wisse, 2004). However, and perhaps surprisingly, in this study, the obesogenic nutrition did not affect cytokines secretion despite the changes in the metabolic parameters. This is possibly due to the short duration of the diet (7 weeks), which may have not been sufficient to cause a severe state of systemic inflammation. Additionally, a previous study suggested that initiating HFD in 6 weeks old mice may not induce a pronounced systemic inflammatory response (Bailey-Downs et al., 2013). Nevertheless, TNF-α and IL-6 levels did increase following the exposure to water soluble PM extracts regardless of the diet, emphasizing the impact of the PM on these markers. We do not rule

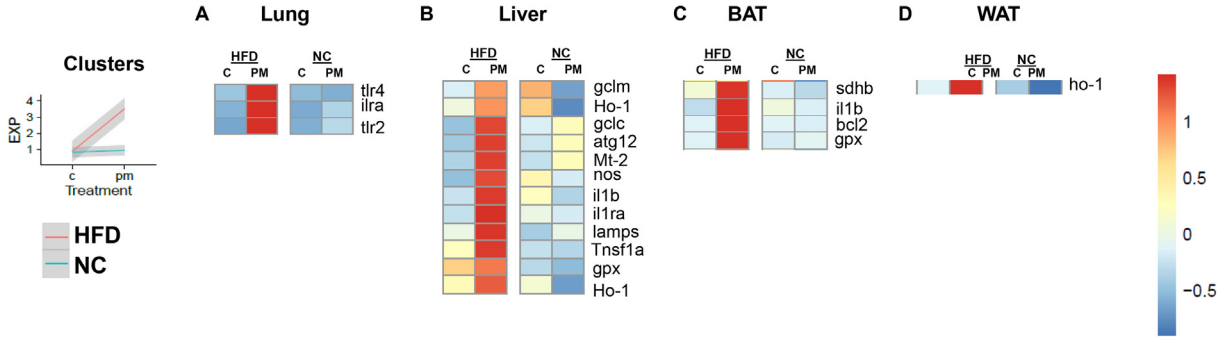

Fig. 4. Genes that were changed as a results of the co-influence of HFD and PM is presented using heat maps in the lung, liver, and adipose tissues (BAT and WAT). The legend on the right indicates expression levels: red color indicates higher expression; blue color indicates lower expression. The names of the genes presented in the right panel of the heatmap are statistically significant at $p < 0.05$. the statistical cluster presented on the left indicates general behavior of genes that were changed after co interaction of HFD (in red line) and NC (in blue line) in the presence of PM.

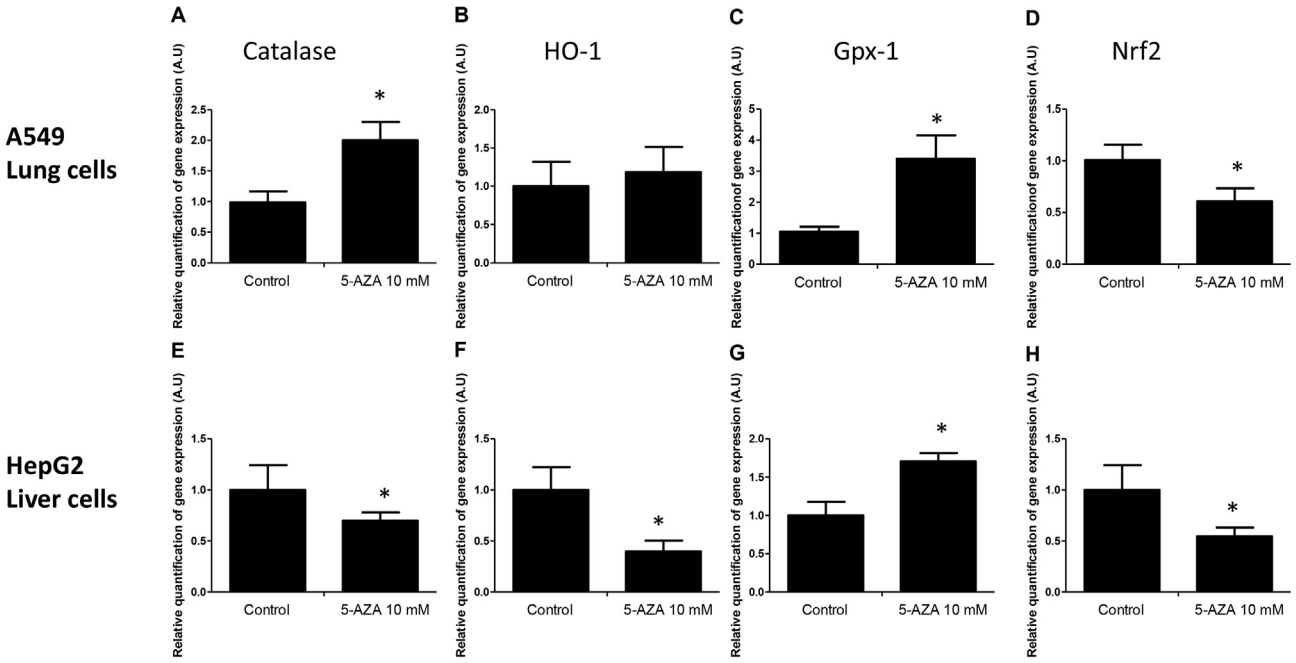

Fig. 5. Inhibition of methylation by 5-Aza-dC influence Nrf2 and related genes expression in lung and liver cells. A549 human lung epithelial cells, and HepG2 human liver carcinoma cells, were treated with 5-Aza-dC as described in the materials and methods. Then the cells were subjected to qPCR for (A, E) Catalase (B, F) HO-1 (C, G) Gpx-1 and (D, H) Nrf2. Values are expressed as fold change of gene expression compared to a calibrator (endogenous controls, HPRT and β-Actin). Data represents two independent experiments, means ± SD; $n = 3$ in each experiment; * significantly higher or lower at $p < 0.05$ than their controls.

out the involvement of other cytokines such as IL-4, IL-5, IL-10, IL-12, IL-13 (Schmidt et al., 2015), that were not measured here, but may be relevant to obesity-induced inflammation.

A master regulator of cells' response to stress is the Nrf2 transcription factor that enhances transcription of cyto-protective genes (Turpaev, 2013). The genes chosen in this study focus on the Nrf2 signaling pathway and on other signal transduction mechanisms such as inflammation and cell death, with an expected partial overlap in the response pathways to either metabolic or PM-exposure challenges. Pre-selection of genes related to the Nrf2 pathway is somehow biased. Therefore, an unbiased statistical bioinformatics analysis was employed to identify gene change patterns in the different tissues.

Interestingly, the 7 weeks HFD increased the expression of Nrf2 related genes in the lungs ("Response to stress" cluster), possibly as a protective process. This is also supported by an observation that synthetic Nrf2 activator can inhibit the onset of obesity (Shin et al., 2009). However, the combined effect of HFD and PM exposure led to a significant decrease in the Nrf2 pathway and related genes. Interestingly, this effect was observed, though to a lesser extent, also in NC fed mice. This observation is interesting in view of our recent finding that mice exposed repeatedly to extracts of the same samples reduced the expression of Nrf2 system, whereas in response to a single exposure activated Nrf2-related response was observed (Pardo et al., 2016). Also, in chronic obstructive pulmonary disease (COPD) model, under high levels of oxidative stress in bronchial epithelial cells, the Nrf2 protein stability and anti-oxidant potential are reduced, possibly contributing to the pathogenesis of COPD (Mercado et al., 2011). Nevertheless, several inflammatory genes (*tlr2, tlr4, and ilra*) (Cantone et al., 2017; Wei et al., 2016), were activated when exposed to PM and obesogenic nutrition. Recently we have shown that exposure to the same water soluble PM sample increased the inflammatory response in mice's lung with increased cell count and neutrophiles number (Pardo et al., 2016). It is postulated that inflammatory activation in the lung through recruitment of inflammatory cells or gene induction can leak out systematically and lead to secondary harmful effects in remote tissues. The lower antioxidant defense and higher inflammatory response in the lungs in the HFD PM mice suggests decompensation of defense mechanisms in the lungs that are the first organ to encounter damaging particles and substances from PM. Therefore, it is reasonable to predict that PM's main adverse influence will be noted in the lungs.

As the effects of inhaled particles can extend beyond the lungs to other organs, including the brain, liver, kidney, spleen, and testes (Li et al., 2017), we examined the effect on remote metabolic tissues such as liver and adipose tissues (WAT and BAT). The exposure to the soluble PM extracts lead to opposite responses (in selected genes) in the lung, (the primary exposure organ) and the liver (secondary exposure organ). The HFD increased *nrf2* and *catalase* genes in the liver compared to the normal diet. Recent studies that focused on the role of Nrf2 in obesity, prediabetes and diabetes, showed that with genetic activation of Nrf2 (manipulation through Kelch-like ECH-associated protein 1, Keap1), β-cells function and insulin sensitivity were protected and suppressed the onset of diabetes (Uruno et al., 2013). Exposure to PM2.5 may activate the Nrf2 system *in vivo* (Chen and Schwartz, 2008; Pardo et al., 2016; Zhang et al., 2012) and *in vitro* (Deng et al., 2013; Lin et al., 2016). In our study, exposure to the PM3 extracts increased the expression of Nrf2 pathway-related genes in the liver and in adipose tissues regardless of the diet (Fig. 4B). Similar behavior was observed in a study reporting that chronic exposure to PM2.5 resulted in impaired glucose tolerance, insulin resistance, inflammation, and stimulated the expression of Nrf2 in WAT and BAT (Xu et al., 2011). Together, the data presented here for the lungs, the liver and the adipose tissues provide general insights into the systemic and tissue-selective impacts of PM2.5 exposure and its possible metabolic implications.

A significant increase in *mt-2* gene expression (a metal carrier, related to protection against metal toxicity (Klaren et al., 2016)) was

observed in the liver following exposure to the PM extracts. This increase was observed under both diets, but to a greater extent under the HFD. Our water soluble PM extracts were rich in soluble metals such as Cd, Cu, Co and Ni (Shuster-Meiseles et al., 2016) that are known to influence MT-2 expression (Sato and Kondoh, 2002). Additionally, in our previous studies we have identified that the dissolved metals in these extracts were the main drivers of PM effects (Pardo et al., 2015). This observation further reinforces the thought that there is a translocation of particles or toxic agents from the respiratory system to other secondary organs, in particular – the liver.

Exposure to pollution particles activates redox-sensitive transcription factors and the MAPK pathways (Pourazar et al., 2005; Wang et al., 2017), suggesting the possible involvement in human respiratory diseases by ROS mediators. In the context of obesity, high circulating levels of pro-inflammatory cytokines (TNFα and IL-1β) and ROS, activate JNK signaling in insulin target cells (Liu et al., 2014; Pal et al., 2013; Vallerie et al., 2008). In the current study, the combination of HFD and exposure to PM influenced genes related to the MAP kinase signaling cluster, especially in the liver and in the adipose tissues. Additionally, the insulin receptor substrate-1 (*irs-1)* gene levels increased in HFD PM mice while its function is known to be impaired in subjects with insulin resistance (Lavin et al., 2016; Schmitz-Peiffer and Whitehead, 2003). At the molecular level, the mice probably did not develop resistance to insulin, as little change was observed in the fed glucose levels examined after the exposure to the water extracts PM. However, this example represents the initiation of the exacerbating effects of HFD on PM exposure. These findings may direct the focus towards the molecular mechanisms of exposure to air pollution and the metabolic abnormalities.

High level gene regulation such as DNA methylation (Yara et al., 2015), histone modification, and microRNAs (Li et al., 2013) are involved in responses to oxidative stress, where DNA methylation specifically plays a key role (Guo et al., 2015; Yara et al., 2015). Our cell-line experiments support epigenetic regulation of the Nrf2 and *catalase* genes. Analysis of the promoter region of Nrf2 gene, 500bp upstream the transcription start site, revealed a CpG island. In addition, a single CpG site was localized 101 base pairs downstream of the transcription start site in the *catalase* promotor (Konki et al., 2016). The overarching differences observed between the lung and liver tissues and cells with the opposite behavior of the "Response to stress" cluster or *catalase* and *ho-1* expression, respectively, may be attributed, at least in part, to changes with DNMT-3a2, a gene we found to be significantly modified in a tissue-specific manner by the exposure (Fig. 6). It is possible that high DNMT-3a2 levels can result hyper-methylation of the CpG island in the Nrf2 and catalase promoter regions. Changes in DNA methylation were already observed in response to PM exposure (Panni et al., 2016) as well as in the Metabolic Syndrome (e.g. obesity, diabetes and hypertension) (Kowluru and Mishra, 2017; Portha et al., 2014; Yara et al., 2015). This may suggest that DNA methylation is a possible high level gene regulation mechanism by which PM and/or diet stress influence Nrf2 and *catalase* response (Fig. 7).

The different tissues examined in this study exhibited different responses to the two stressors (Fig. 7). Metabolic tissues that intuitively are not expected to be influenced by the exposure to PM exhibited changes in gene expression following the exposure. Significant changes in gene expression profile were observed in the lung, a tissue that is not intuitively expected to be influenced by obesogenic diet. For some genes, the HFD exacerbated the effect of exposure, especially when related to response to stress or inflammation. Consistently with our previous studies (Pardo et al., 2015, 2016; Shuster-Meiseles et al., 2016), we suggest that in lung cells, the direct exposure to toxic doses of inhaled extracts and their components exceeds the capacity of the lungs' protective

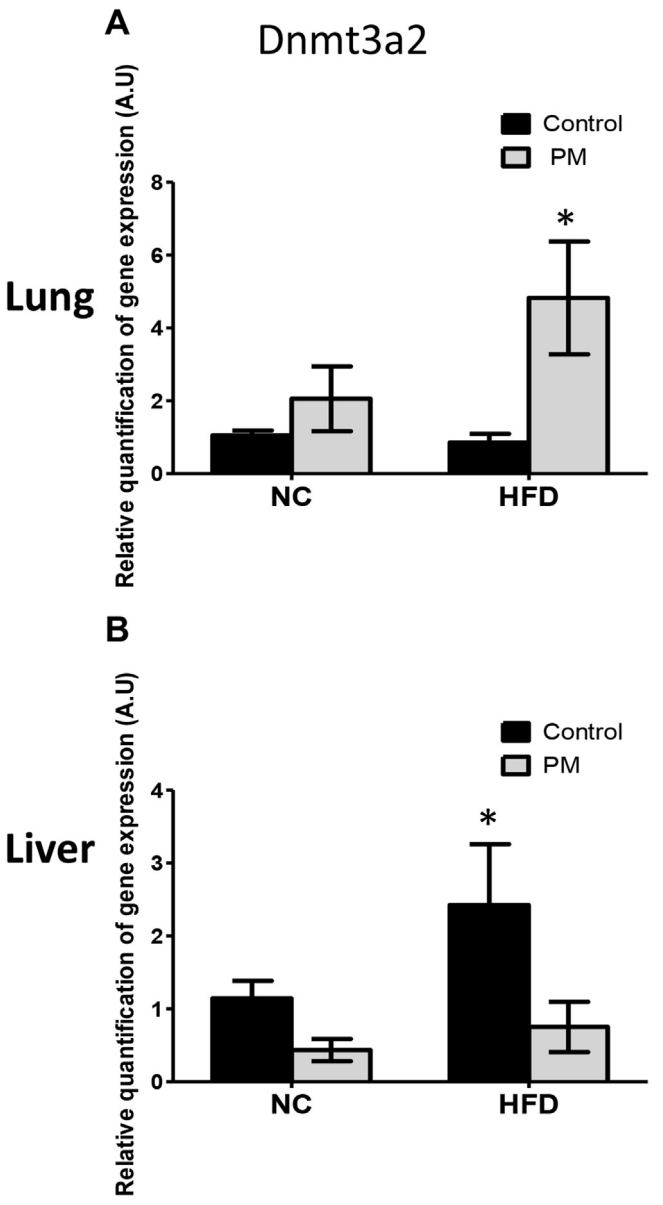

Fig. 6. Transcription levels of DNA methyltransferase 3a-2 (DNMT3a-2) enzyme in the lung and liver following exposure to PM in mice. Quantitative analysis of DNMT3a-2 in the lung (A) and liver (B). Values are expressed as fold change of gene expression compared to a calibrator (endogenous controls, HPRT and β-Actin). Data represent means ± SE; $n = 5$ mice per group; * significantly higher or lower at $p < 0.05$ than their controls.

mechanisms (e.g *catalase*, Nrf2 and related genes), resulting in their suppression (Fig. 7). As a secondary response, inflammatory mediators, or the toxic components themselves, translocate through the blood circulation to other organs and induce the activation of protective mechanisms. In the secondary organs, the toxic dose is substantially lower. In addition, gene methylation is suggested to influence the response to oxidative stress and the expression of *catalase* and Nrf2, in a unique manner in the studied tissues possibly through the mediation of DNAMT-3a2. Therefore, we suggest that oxidative stress and inflammation in combination with epigenetic variations has a systems-level effect on different organs or tissues especially on the role of catalase and Nrf2. This may synergistically contribute to the mechanism by which exposure to water soluble PM increases insulin resistance in obese subjects.

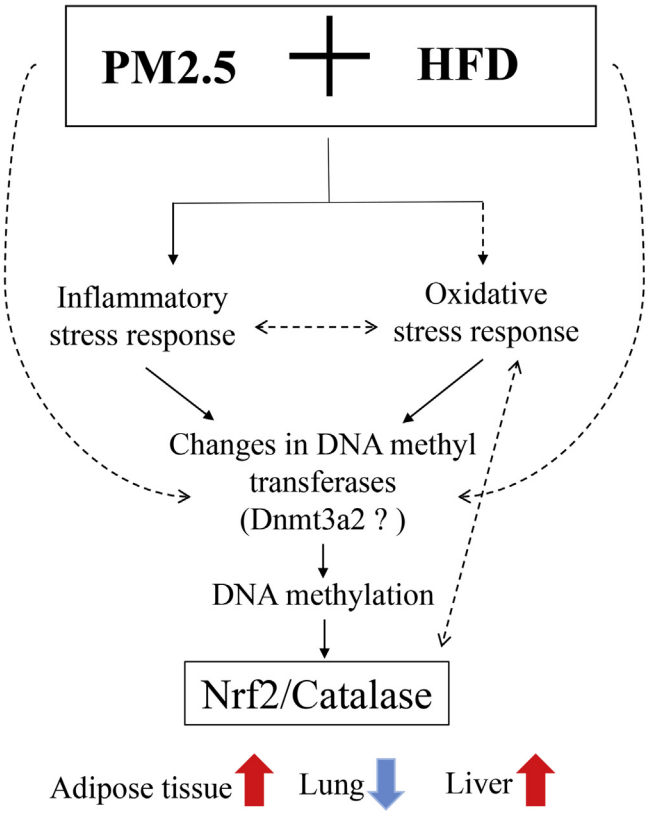

Fig. 7. Possible signaling cascade derived from the combination of PM and HFD. Exposure to obesogenic diet and air pollution increases inflammation and oxidative stress, the latter triggered epigenetic changes leading to diverse responses of Nrf2 transcription factor and or catalase in the tissues. Dashed lines are other connections that were not tested directly in this work.

Understanding the complexity, organ-specific, cellular response and defense mechanisms may provide potential new therapeutic approaches for disease prevention. Further studies are required to elucidate the mechanisms involved in obesity and exposure to PM in a tissue specific manner.

Acknowledgments

Y.K. is the incumbent of the Sarah and Rolando Uziel Research Associate Chair. We thank Dr. Yoav Barak and Sharon Manashirov for their fruitful discussions. This research was partially funded by the Israel Science Foundation (ISF) and the National Natural Science Foundation of China (NSFC) grant number 2229/15. A.R. and J.J.S. collaboration was supported by the Israel–US Binational Science Foundation (BSF) 20111/78.

Appendix A. Supplementary data

Supplementary data related to this article can be found at https://doi.org/10.1016/j.envpol.2018.04.048.

Competing financial interests

None.

Unlisted references

Yang et al., 2018.

References

Axelsen, L.N., Calloe, K., Braunstein, T.H., Riemann, M., Hofgaard, J.P., Liang, B., Jensen, C.F., Olsen, K.B., Bartels, E.D., Baandrup, U., Jespersen, T., Nielsen, L.B., Holstein-Rathlou, N.H., Nielsen, M.S., 2015. Diet-induced pre-diabetes slows cardiac conductance and promotes arrhythmogenesis. Cardiovasc. Diabetol. 14, 87.

Bailey-Downs, L.C., Tucsek, Z., Toth, P., Sosnowska, D., Gautam, T., Sonntag, W.E., Csiszar, A., Ungvari, Z., 2013. Aging exacerbates obesity-induced oxidative stress and inflammation in perivascular adipose tissue in mice: a paracrine mechanism contributing to vascular redox dysregulation and inflammation. J. Gerontol. A Biol. Sci. Med. Sci. 68, 780–792.

Bennett, W.D., Zeman, K.L., 2004. Effect of body size on breathing pattern and fine-particle deposition in children. J. Appl. Physiol. 97, 821–826 (1985).

Bide, W., Armour, R.J., Yee, E, S., 1997. Estimation of Human Toxicity from Animal Inhalation Toxicity Data: 1. Minute Volume-Body Weight Relationships between Animals and Man suffield report 673, Alberta: Defence Research Establishment Suffieled, Alberta.

Brook, R.D., Xu, X., Bard, R.L., Dvonch, J.T., Morishita, M., Kaciroti, N., Sun, Q., Harkema, J., Rajagopalan, S., 2013. Reduced metabolic insulin sensitivity following sub-acute exposures to low levels of ambient fine particulate matter air pollution. Sci. Total Environ. 448, 66–71.

Cantone, L., Iodice, S., Tarantini, L., Albetti, B., Restelli, I., Vigna, L., Bonzini, M., Pesatori, A.C., Bollati, V., 2017. Particulate matter exposure is associated with inflammatory gene methylation in obese subjects. Environ. Res. 152, 478–484.

Chen, J.C., Schwartz, J., 2008. Metabolic syndrome and inflammatory responses to long-term particulate air pollutants. Environ. Health Perspect. 116, 612–617.

Chen, A., Brar, B., Choi, C.S., Rousso, D., Vaughan, J., Kuperman, Y., Kim, S.N., Donaldson, C., Smith, S.M., Jamieson, P., Li, C., Nagy, T.R., Shulman, G.I., Lee, K.F., Vale, W., 2006. Urocortin 2 modulates glucose utilization and insulin sensitivity in skeletal muscle. Proc. Natl. Acad. Sci. U. S. A. 103, 16580–16585.

Collaborators, G.B.D.R.F., 2016. Global, regional, and national comparative risk assessment of 79 behavioural, environmental and occupational, and metabolic risks or clusters of risks, 1990-2015: a systematic analysis for the Global Burden of Disease Study 2015. Lancet 388, 1659–1724.

Cui, Y., Jia, F., He, J., Xie, X., Li, Z., Fu, M., Hao, H., Liu, Y., Liu, D.Z., Cowan, P.J., Zhu, H., Sun, Q., Liu, Z., 2015. Ambient fine particulate matter suppresses in vivo proliferation of bone marrow stem cells through reactive oxygen species formation. PLoS One 10 e0127309.

Deng, X., Rui, W., Zhang, F., Ding, W., 2013. PM2.5 induces Nrf2-mediated defense mechanisms against oxidative stress by activating PIK3/AKT signaling pathway in human lung alveolar epithelial A549 cells. Cell Biol. Toxicol. 29, 143–157.

Dong, G.H., Qian, Z., Liu, M.M., Wang, D., Ren, W.H., Fu, Q., Wang, J., Simckes, M., Ferguson, T.F., Trevathan, E., 2013. Obesity enhanced respiratory health effects of ambient air pollution in Chinese children: the Seven Northeastern Cities study. Int. J. Obes. 37, 94–100.

Dubowsky, S.D., Suh, H., Schwartz, J., Coull, B.A., Gold, D.R., 2006. Diabetes, obesity, and hypertension may enhance associations between air pollution and markers of systemic inflammation. Environ. Health Perspect. 114, 992–998.

Fernandez-Sanchez, A., Madrigal-Santillan, E., Bautista, M., Esquivel-Soto, J., Morales-Gonzalez, A., Esquivel-Chirino, C., Durante-Montiel, I., Sanchez-Rivera, G., Valadez-Vega, C., Morales-Gonzalez, J.A., 2011. Inflammation, oxidative stress, and obesity. Int. J. Mol. Sci. 12, 3117–3132.

Fischer, B.M., Neumann, D., Piberger, A.L., Risnes, S.F., Koberle, B., Hartwig, A., 2016. Use of high-throughput RT-qPCR to assess modulations of gene expression profiles related to genomic stability and interactions by cadmium. Arch. Toxicol. 90, 2745–2761.

Fisher-Wellman, K.H., Ryan, T.E., Smith, C.D., Gilliam, L.A., Lin, C.T., Reese, L.R., Torres, M.J., Neufer, P.D., 2016. A direct comparison of metabolic responses to high-fat diet in C57BL/6J and C57BL/6NJ mice. Diabetes 65, 3249–3261.

Giacco, F., Brownlee, M., 2010. Oxidative stress and diabetic complications. Circ. Res. 107, 1058–1070.

Guo, Y., Yu, S., Zhang, C., Kong, A.N., 2015. Epigenetic regulation of Keap1-Nrf2 signaling. Free Radic. Biol. Med. 88, 337–349.

Haberzettl, P., O'Toole, T.E., Bhatnagar, A., Conklin, D.J., 2016. Exposure to fine particulate air pollution causes vascular insulin resistance by inducing pulmonary oxidative stress. Environ. Health Perspect. 124, 1830–1839.

Hochberg, Y., 1988. A Sharper Bonferroni Procedure for Multiple Tests of Significance.

Hooper, P.L., Balogh, G., Rivas, E., Kavanagh, K., Vigh, L., 2014. The importance of the cellular stress response in the pathogenesis and treatment of type 2 diabetes. Cell Stress Chaperones 19, 447–464.

Houstis, N., Rosen, E.D., Lander, E.S., 2006. Reactive oxygen species have a causal role in multiple forms of insulin resistance. Nature 440, 944–948.

Huang da, W., Sherman, B.T., Lempicki, R.A., 2009. Systematic and integrative analysis of large gene lists using DAVID bioinformatics resources. Nat. Protoc. 4, 44–57.

Jimenez-Osorio, A.S., Gonzalez-Reyes, S., Pedraza-Chaverri, J., 2015. Natural Nrf2 activators in diabetes. Clin. Chim. Acta 448, 182–192.

Kampfrath, T., Maiseyeu, A., Ying, Z., Shah, Z., Deiuliis, J.A., Xu, X., Kherada, N., Brook, R.D., Reddy, K.M., Padture, N.P., Parthasarathy, S., Chen, L.C., Moffatt-Bruce, S., Sun, Q., Morawietz, H., Rajagopalan, S., 2011. Chronic fine particulate matter exposure induces systemic vascular dysfunction via NADPH oxidase and TLR4 pathways. Circ. Res. 108, 716–726.

Kensler, T.W., Wakabayashi, N., Biswal, S., 2007. Cell survival responses to environmental stresses via the Keap1-Nrf2-ARE pathway. Annu. Rev. Pharmacol. Toxicol. 47, 89–116.
Klaren, W.D., Flor, S., Gibson-Corley, K.N., Ludewig, G., Robertson, L.W., 2016. Metallothionein's role in PCB126 induced hepatotoxicity and hepatic micronutrient disruption. Toxicol. Rep. 3, 21–28.
Konki, M., Pasumarthy, K., Malonzo, M., Sainio, A., Valensisi, C., Soderstrom, M., Emani, M.R., Stubb, A., Narva, E., Ghimire, B., Laiho, A., Jarvelainen, H., Lahesmaa, R., Lahdesmaki, H., Hawkins, R.D., Lund, R.J., 2016. Epigenetic silencing of the key antioxidant enzyme catalase in karyotypically abnormal human pluripotent stem cells. Sci. Rep. 6, 22190.
Kowluru, R.A., Mishra, M., 2017. Epigenetic regulation of redox signaling in diabetic retinopathy: role of Nrf2. Free Radic. Biol. Med. 103, 155–164.
Kozera, B., Rapacz, M., 2013. Reference genes in real-time PCR. J. Appl. Genet. 54, 391–406.
Lavin, D.P., White, M.F., Brazil, D.P., 2016. IRS proteins and diabetic complications. Diabetologia 59, 2280–2291.
Li, Y.J., Yu, C.H., Li, J.B., Wu, X.Y., 2013. Andrographolide antagonizes cigarette smoke extract-induced inflammatory response and oxidative stress in human alveolar epithelial A549 cells through induction of microRNA-218. Exp. Lung Res. 39, 463–471.
Li, X.Y., Hao, L., Liu, Y.H., Chen, C.Y., Pai, V.J., Kang, J.X., 2017. Protection against fine particle-induced pulmonary and systemic inflammation by omega-3 polyunsaturated fatty acids. Biochim. Biophys. Acta 1861, 577–584.
Lin, Y.-H., Arashiro, M., Martin, E., Chen, Y., Zhang, Z., Sexton, K.G., Gold, A., Jaspers, I., Fry, R.C., Surratt, J.D., 2016. Isoprene-derived secondary organic aerosol induces the expression of oxidative stress response genes in human lung cells. Environ. Sci. Technol. Lett. 3, 250–254.
Liu, C., Ying, Z., Harkema, J., Sun, Q., Rajagopalan, S., 2013. Epidemiological and experimental links between air pollution and type 2 diabetes. Toxicol. Pathol. 41, 361–373.
Liu, C., Xu, X., Bai, Y., Wang, T.Y., Rao, X., Wang, A., Sun, L., Ying, Z., Gushchina, L., Maiseyeu, A., Morishita, M., Sun, Q., Harkema, J.R., Rajagopalan, S., 2014. Air pollution-mediated susceptibility to inflammation and insulin resistance: influence of CCR2 pathways in mice. Environ. Health Perspect. 122, 17–26.
Liu, T., Wu, B., Wang, Y., He, H., Lin, Z., Tan, J., Yang, L., Kamp, D.W., Zhou, X., Tang, J., Huang, H., Zhang, L., Bin, L., Liu, G., 2015. Particulate matter 2.5 induces autophagy via inhibition of the phosphatidylinositol 3-kinase/Akt/mammalian target of rapamycin kinase signaling pathway in human bronchial epithelial cells. Mol. Med. Rep. 12, 1914–1922.
Lodovici, M., Bigagli, E., 2011. Oxidative stress and air pollution exposure. J. Toxicol.
Matouskova, P., Bartikova, H., Bousova, I., Hanusova, V., Szotakova, B., Skalova, L., 2014. Reference genes for real-time PCR quantification of messenger RNAs and microRNAs in mouse model of obesity. PLoS One 9, e86033.
McCormack, M.C., Belli, A.J., Kaji, D.A., Matsui, E.C., Brigham, E.P., Peng, R.D., Sellers, C., Williams, D.L., Diette, G.B., Breysse, P.N., Hansel, N.N., 2015. Obesity as a susceptibility factor to indoor particulate matter health effects in COPD. Eur. Respir. J. 45, 1248–1257.
McMurray, F., Patten, D.A., Harper, M.E., 2016. Reactive oxygen species and oxidative stress in obesity-recent findings and empirical approaches. Obesity 24, 2301–2310.
Mendez, R., Zheng, Z., Fan, Z., Rajagopalan, S., Sun, Q., Zhang, K., 2013. Exposure to fine airborne particulate matter induces macrophage infiltration, unfolded protein response, and lipid deposition in white adipose tissue. Am. J. Transl. Res. 5, 224–234.
Meo, S.A., Memon, A.N., Sheikh, S.A., Rouq, F.A., Usmani, A.M., Hassan, A., Arian, S.A., 2015. Effect of environmental air pollution on type 2 diabetes mellitus. Eur. Rev. Med. Pharmacol. Sci. 19, 123–128.
Mercado, N., Thimmulappa, R., Thomas, C.M., Fenwick, P.S., Chana, K.K., Donnelly, L.E., Biswal, S., Ito, K., Barnes, P.J., 2011. Decreased histone deacetylase 2 impairs Nrf2 activation by oxidative stress. Biochem. Biophys. Res. Commun. 406, 292–298.
Montgomery, M.K., Hallahan, N.L., Brown, S.H., Liu, M., Mitchell, T.W., Cooney, G.J., Turner, N., 2013. Mouse strain-dependent variation in obesity and glucose homeostasis in response to high-fat feeding. Diabetologia 56, 1129–1139.
Nygard, A.B., Jorgensen, C.B., Cirera, S., Fredholm, M., 2007. Selection of reference genes for gene expression studies in pig tissues using SYBR green qPCR. BMC Mol. Biol. 8, 67.
Okano, M., Bell, D.W., Haber, D.A., Li, E., 1999. DNA methyltransferases Dnmt3a and Dnmt3b are essential for de novo methylation and mammalian development. Cell 99, 247–257.
Pal, S., Blais, J.M., Robidoux, M.A., Haman, F., Krummel, E., Seabert, T.A., Imbeault, P., 2013. The association of type 2 diabetes and insulin resistance/secretion with persistent organic pollutants in two First Nations communities in northern Ontario. Diabetes Metab. 39, 497–504.
Panni, T., Mehta, A.J., Schwartz, J.D., Baccarelli, A.A., Just, A.C., Wolf, K., Wahl, S., Cyrys, J., Kunze, S., Strauch, K., Waldenberger, M., Peters, A., 2016. Genome-wide analysis of DNA methylation and fine particulate matter air pollution in three study populations: KORA F3, KORA F4, and the normative aging study. Environ. Health Perspect. 124, 983–990.
Pardo, M., Shafer, M.M., Rudich, A., Schauer, J.J.a.R., Y., 2015. Single exposure to near roadway particulate matter leads to confined inflammatory and defense responses: possible role of metals from non-tailpipe roadway sources (submitted). Environ. Sci. Technol.
Pardo, M., Porat, Z., Rudich, A., Schauer, J.J., Rudich, Y., 2016. Repeated exposures to roadside particulate matter extracts suppresses pulmonary defense mechanisms, resulting in lipid and protein oxidative damage. Environ. Pollut. 210, 227–237.
Pearson, J.F., Bachireddy, C., Shyamprasad, S., Goldfine, A.B., Brownstein, J.S., 2010. Association between fine particulate matter and diabetes prevalence in the U.S. Diabetes Care 33, 2196–2201.
Portha, B., Fournier, A., Kioon, M.D., Mezger, V., Movassat, J., 2014. Early environmental factors, alteration of epigenetic marks and metabolic disease susceptibility. Biochimie 97, 1–15.
Pourazar, J., Mudway, I.S., Samet, J.M., Helleday, R., Blomberg, A., Wilson, S.J., Frew, A.J., Kelly, F.J., Sandstrom, T., 2005. Diesel exhaust activates redox-sensitive transcription factors and kinases in human airways. Am. J. Physiol. Lung Cell Mol. Physiol. 289, L724–L730.
Ray, P.D., Huang, B.W., Tsuji, Y., 2012. Reactive oxygen species (ROS) homeostasis and redox regulation in cellular signaling. Cell. Signal. 24, 981–990.
Sato, M., Kondoh, M., 2002. Recent studies on metallothionein: protection against toxicity of heavy metals and oxygen free radicals. Tohoku J. Exp. Med. 196, 9–22.
Savini, I., Catani, M.V., Evangelista, D., Gasperi, V., Avigliano, L., 2013. Obesity-associated oxidative stress: strategies finalized to improve redox state. Int. J. Mol. Sci. 14, 10497–10538.
Schmidt, F.M., Weschenfelder, J., Sander, C., Minkwitz, J., Thormann, J., Chittka, T., Mergl, R., Kirkby, K.C., Fasshauer, M., Stumvoll, M., Holdt, L.M., Teupser, D., Hegerl, U., Himmerich, H., 2015. Inflammatory cytokines in general and central obesity and modulating effects of physical activity. PLoS One 10 e0121971.
Schmitz-Peiffer, C., Whitehead, J.P., 2003. IRS-1 regulation in health and disease. IUBMB Life 55, 367–374.
Shin, S., Wakabayashi, J., Yates, M.S., Wakabayashi, N., Dolan, P.M., Aja, S., Liby, K.T., Sporn, M.B., Yamamoto, M., Kensler, T.W., 2009. Role of Nrf2 in prevention of high-fat diet-induced obesity by synthetic triterpenoid CDDO-imidazolide. Eur. J. Pharmacol. 620, 138–144.
Shuster-Meiseles, T., Shafer, M.M., Heo, J., Pardo, M., Antkiewicz, D.S., Schauer, J.J., Rudich, A., Rudich, Y., 2016. ROS-generating/ARE-activating capacity of metals in roadway particulate matter deposited in urban environment. Environ. Res. 146, 252–262.
Turpaev, K.T., 2013. Keap1-Nrf2 signaling pathway: mechanisms of regulation and role in protection of cells against toxicity caused by xenobiotics and electrophiles. Biochemistry (Mosc.) 78, 111–126.
Uruno, A., Furusawa, Y., Yagishita, Y., Fukutomi, T., Muramatsu, H., Negishi, T., Sugawara, A., Kensler, T.W., Yamamoto, M., 2013. The Keap1-Nrf2 system prevents onset of diabetes mellitus. Mol. Cell Biol. 33, 2996–3010.
Vallerie, S.N., Furuhashi, M., Fucho, R., Hotamisligil, G.S., 2008. A predominant role for parenchymal c-Jun amino terminal kinase (JNK) in the regulation of systemic insulin sensitivity. PLoS One 3, e3151.
Wang, R., Xiao, X., Shen, Z., Cao, L., Cao, Y., 2017. Airborne fine particulate matter causes murine bronchial hyperreactivity via MAPK pathway-mediated M3 muscarinic receptor upregulation. Environ. Toxicol. 32, 371–381.
Wei, Y., Zhang, J.J., Li, Z., Gow, A., Chung, K.F., Hu, M., Sun, Z., Zeng, L., Zhu, T., Jia, G., Li, X., Duarte, M., Tang, X., 2016. Chronic exposure to air pollution particles increases the risk of obesity and metabolic syndrome: findings from a natural experiment in Beijing. Faseb. J.. 30, 2115–2122.
Wisse, B.E., 2004. The inflammatory syndrome: the role of adipose tissue cytokines in metabolic disorders linked to obesity. J. Am. Soc. Nephrol. 15, 2792–2800.
Xu, Z., Xu, X., Zhong, M., Hotchkiss, I.P., Lewandowski, R.P., Wagner, J.G., Bramble, L.A., Yang, Y., Wang, A., Harkema, J.R., Lippmann, M., Rajagopalan, S., Chen, L.C., Sun, Q., 2011. Ambient particulate air pollution induces oxidative stress and alterations of mitochondria and gene expression in brown and white adipose tissues. Part. Fibre Toxicol. 8, 20.
Yang, B.-Y., Qian, Z., Li, S., Chen, G., Bloom, M.S., Elliott, M., Syberg, K.W., Heinrich, J., Markevych, I., Wang, S.-Q., Chen, D., Ma, H., Chen, D.-H., Liu, Y., Komppula, M., Leskinen, A., Liu, K.-K., Zeng, X.-W., Hu, L.-W., Guo, Y., Dong, G.-H., 2018. Ambient air pollution in relation to diabetes and glucose-homoeostasis markers in China: a cross-sectional study with findings from the 33 Communities Chinese Health Study. Lancet Planet. Health 2, e64–e73.
Yara, S., Lavoie, J.C., Levy, E., 2015. Oxidative stress and DNA methylation regulation in the metabolic syndrome. Epigenomics 7, 283–300.
Zanobetti, A., Dominici, F., Wang, Y., Schwartz, J.D., 2014. A national case-crossover analysis of the short-term effect of PM2.5 on hospitalizations and mortality in subjects with diabetes and neurological disorders. Environ. Health 13, 38.
Zhang, H., Liu, H., Davies, K.J., Sioutas, C., Finch, C.E., Morgan, T.E., Forman, H.J., 2012. Nrf2-regulated phase II enzymes are induced by chronic ambient nanoparticle exposure in young mice with age-related impairments. Free Radic. Biol. Med. 52, 2038–2046.